IBM Research

# *In-situ* and Other X-ray Diffraction Techniques Applicable to Photocathode Materials Research

**Jean Jordan-Sweet (IBM X20)**

**Karl Ludwig (Boston University, X21)**

**Randall Headrick (University of Vermont, X21)**

# Outline

- **Motivation:**

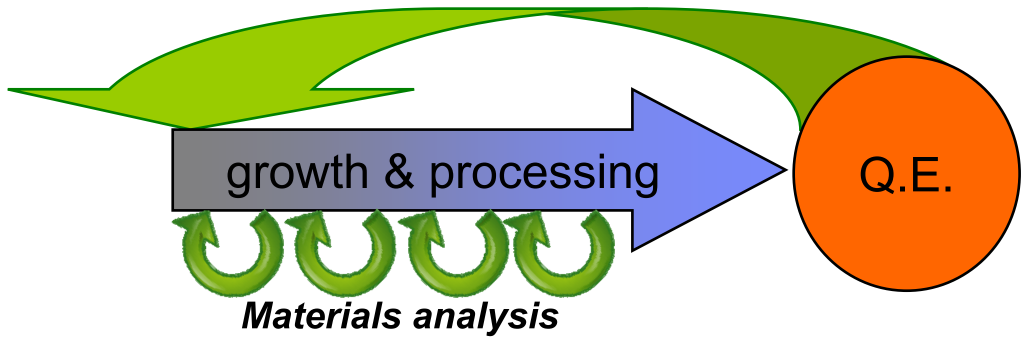


- **Background**
  - crystal planes, diffraction, diffractometers, *etc*.
- **Standard XRD techniques for “stable” materials**
  - Phase ID, grain size, texture, strain
- **Special XRD techniques for reactive materials**
  - *In-situ* thermal processing (phase formation, grain growth) –X20C
  - *In-situ* growth and processing – X21

# Crystals and crystal planes

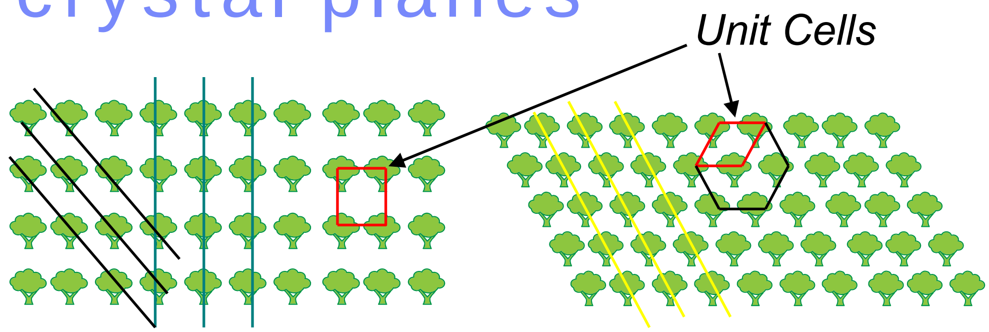


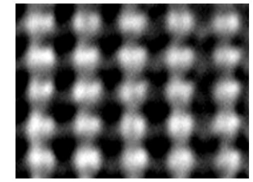

Atoms of silicon
spacing 0.078 nm

## *Miller Indices (h k l)*

If *x, y, z are the fractional coordinates of the intersections of the plane with* **a**, **b**, **c,** Miller indices are the smallest integers in the same ratio as (1/x, 1/y, 1/z).

*The "hkl" direction is orthogonal to the hkl planes*

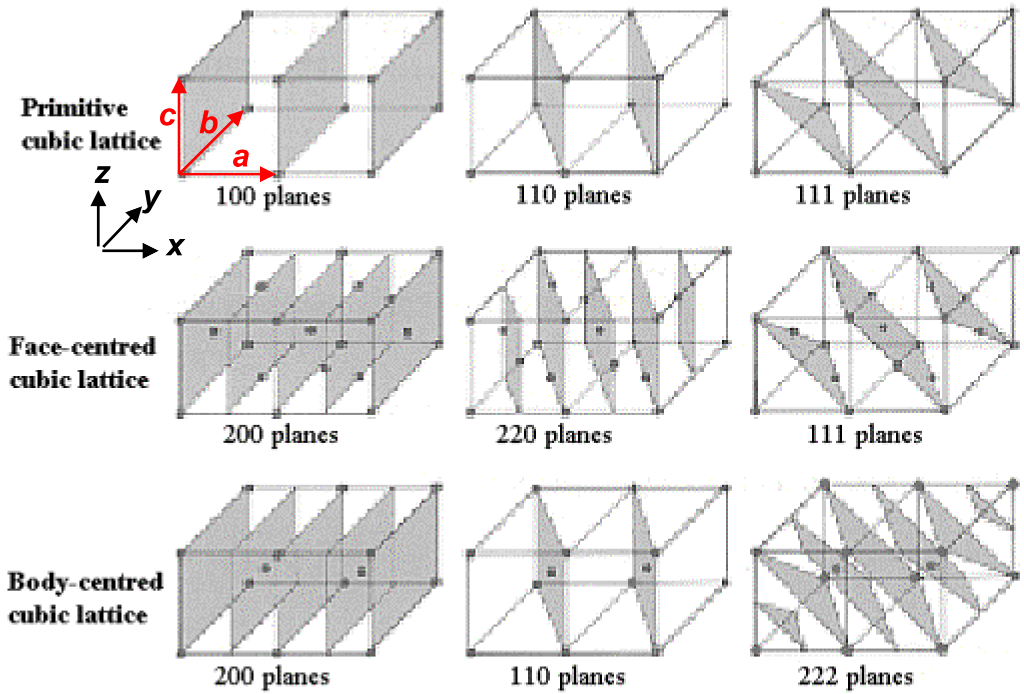


Miller indices for three types of cubic lattices.

*theochem.unito.it*

# X-ray Diffraction

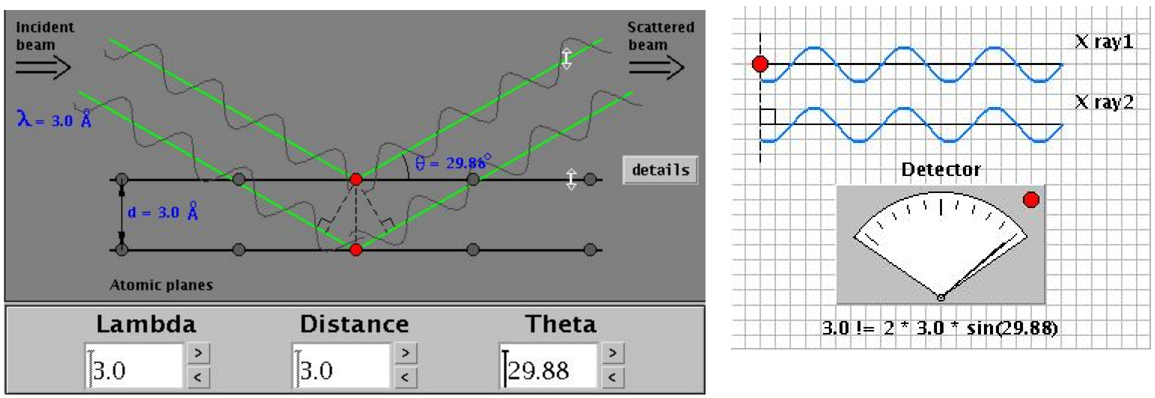


Constructive interference:(waves match up)

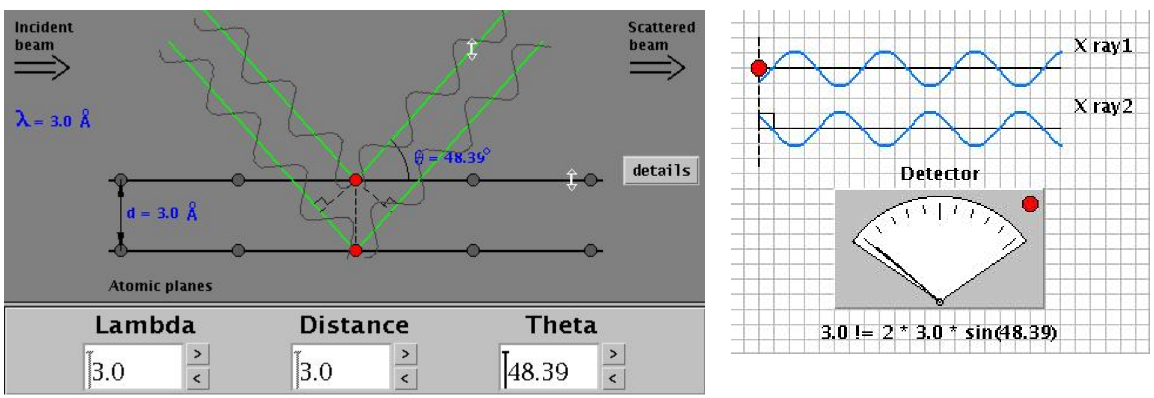


Destructive interference:(waves don't match up)

***Bragg's Law:***
$$n\lambda = 2d \sin\theta$$

$$q = (4\pi/\lambda) \sin\theta$$
$$q = 2\pi/d$$

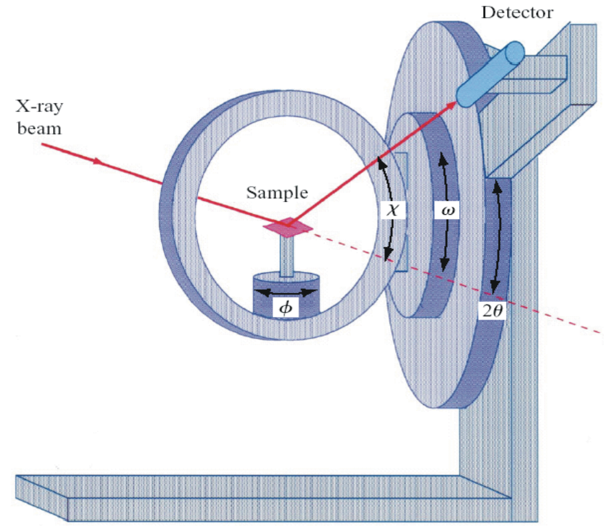


***4-circle diffractometer***

*http://www.eserc.stonybrook.edu/ProjectJava/Bragg*

B.D. Cullity, Elements of X-ray Diffraction

# High-resolution (triple-axis) XRD

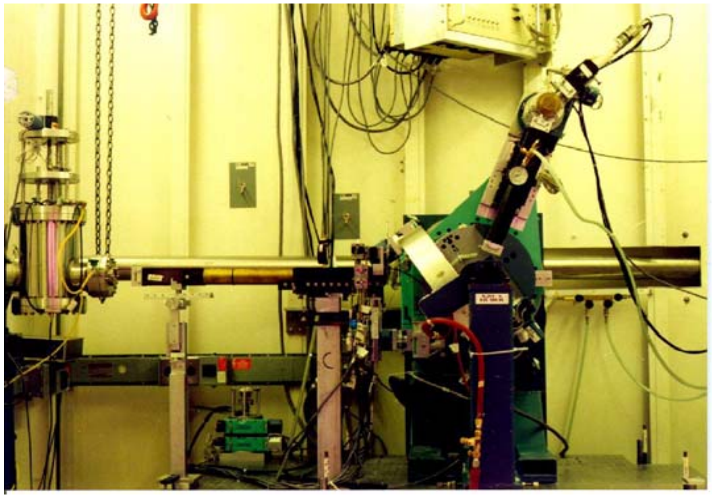

Triple-axis configuration in NSLS X20A hutch

- Crystalline materials
- Radial scans> lattice spacing
  - Strain
  - Phase ID
  - Crystallite size
- Omega (theta) scans> orientation
- Reciprocal space maps

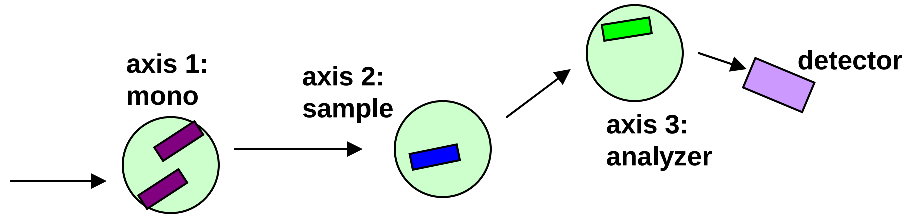


## *Phase ID example: cubic vs. tetragonal $BaTiO_3$*

**PDF # 792263, Wavelength = 1.54060 (A)**

79-2263 Quality: C
CAS Number:
Molecular Weight: 233.23
Volume[CD]: 64.29
Dx: 6.024 Dm:
S.G.: Pm3m (221)
Cell Parameters:
a 4.006 b c
α β γ
I/Icor: 11.49
Rad: CuKa1
Lambda: 1.54060
Filter:
d-sp: calculated
ICSD # : 067518

Ba ( Ti O3 )
Barium Titanium Oxide
Ref: Calculated from ICSD using POWD-12++, (1997)
Ref: Buttner, R.H., Maslen, E.N., Acta Crystallogr., Sec. B: Structural Science, 48, 764 (1992)

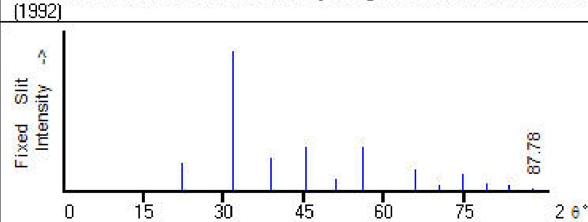


| 2θ | Int-f | h | k | l | 2θ | Int-f | h | k | l | 2θ | Int-f | h | k | l |
|---|---|---|---|---|---|---|---|---|---|---|---|---|---|---|
| 22.173 | 202 | 1 | 0 | 0 | 50.931 | 85 | 2 | 1 | 0 | 74.899 | 115 | 3 | 1 | 0 |
| 31.559 | 999 | 1 | 1 | 0 | 56.199 | 315 | 2 | 1 | 1 | 79.248 | 56 | 3 | 1 | 1 |
| 38.908 | 234 | 1 | 1 | 1 | 65.895 | 151 | 2 | 2 | 0 | 83.534 | 43 | 2 | 2 | 2 |
| 45.235 | 307 | 2 | 0 | 0 | 70.460 | 40 | 2 | 2 | 1 | 87.784 | 17 | 3 | 2 | 0 |

**PDF # 831880, Wavelength = 1.54060 (A)**

83-1880 Quality: C
CAS Number:
Molecular Weight: 233.23
Volume[CD]: 64.36
Dx: 6.018 Dm:
S.G.: P4mm (99)
Cell Parameters:
a 3.994 b c 4.033
α β γ
I/Icor: 7.46
Rad: CuKa1
Lambda: 1.54060
Filter:
d-sp: calculated
ICSD # : 100804
Mineral Name:
Perovskite (Ba) - artificial

Ba Ti O3
Barium Titanium Oxide
Ref: Calculated from ICSD using POWD-12++, (1997)
Ref: Waesche, R., Denner, W., Schulz, H., Mater. Res. Bull., 16, 497 (1981)

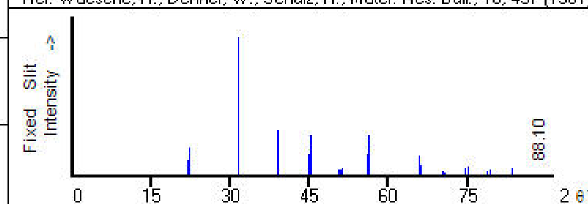


| 2θ | Int-f | h | k | l | 2θ | Int-f | h | k | l | 2θ | Int-f | h | k | l |
|---|---|---|---|---|---|---|---|---|---|---|---|---|---|---|
| 22.019 | 106 | 0 | 0 | 1 | 51.088 | 54 | 2 | 1 | 0 | 75.067 | 59 | 3 | 0 | 1 |
| 22.237 | 201 | 1 | 0 | 0 | 55.980 | 151 | 1 | 1 | 2 | 75.152 | 60 | 3 | 1 | 0 |
| 31.495 | 999 | 1 | 0 | 1 | 56.277 | 291 | 2 | 1 | 1 | 78.769 | 23 | 1 | 1 | 3 |
| 31.652 | 598 | 1 | 1 | 0 | 65.750 | 138 | 2 | 0 | 2 | 79.438 | 45 | 3 | 1 | 1 |
| 38.894 | 329 | 1 | 1 | 1 | 66.109 | 71 | 2 | 2 | 0 | 83.498 | 54 | 2 | 2 | 2 |
| 44.909 | 153 | 0 | 0 | 2 | 69.909 | 4 | 0 | 0 | 3 | 87.363 | 7 | 2 | 0 | 3 |
| 45.372 | 292 | 2 | 0 | 0 | 70.345 | 27 | 2 | 1 | 2 | 87.773 | 7 | 3 | 0 | 2 |
| 50.665 | 39 | 1 | 0 | 2 | 70.606 | 20 | 2 | 2 | 1 | 88.102 | 8 | 3 | 2 | 0 |
| 50.983 | 43 | 2 | 0 | 1 | 74.387 | 51 | 1 | 0 | 3 | | | | | |

# Anomalous self-annealing in Cu films

- Electroplated Cu thin films exhibit room temperature anomalous self-annealing
- Characterized by HRXRD and Cu peak profile fitting
- Samples were 4mm dia plated at 44mA/cm2 for 20-80 sec. on 50 nm Cu seed
- Highly 111 textured, Lorentzian + pseudo-Voigt profile
- 111 grains grow volumetrically initially, then change to planar growth

**80-sec plated sample**

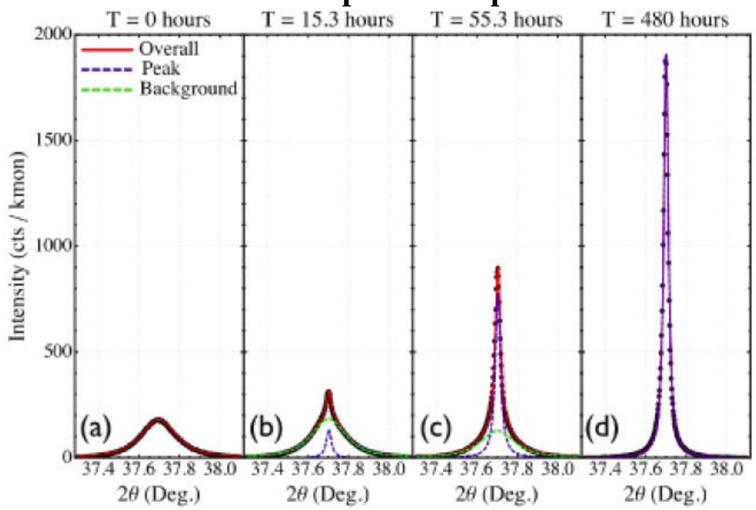


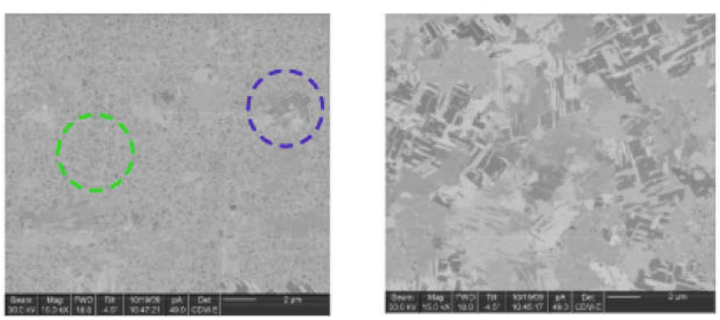

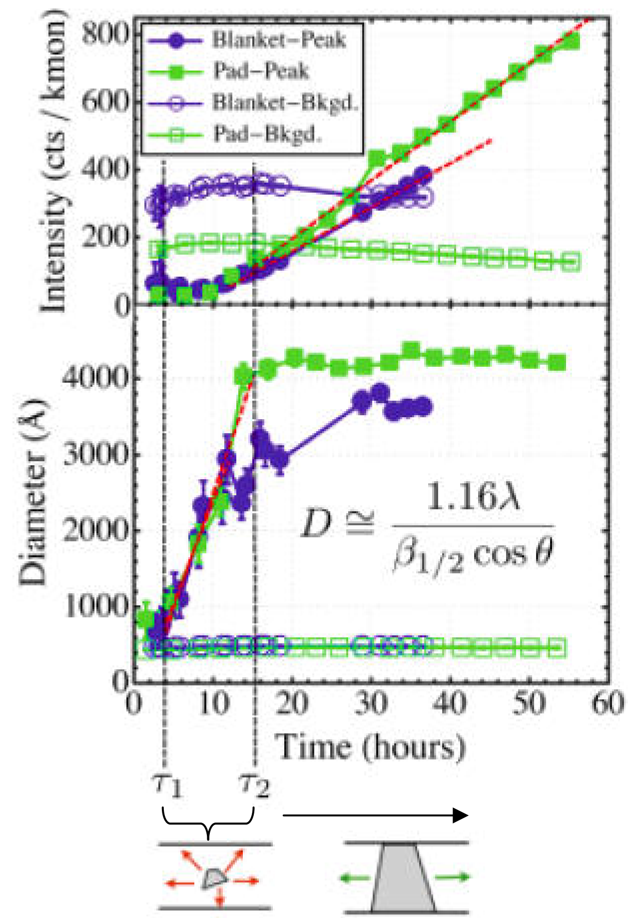


A. Ying, I.C Noyan *et al.,* JAP, in press

# Grazing-incidence Diffraction

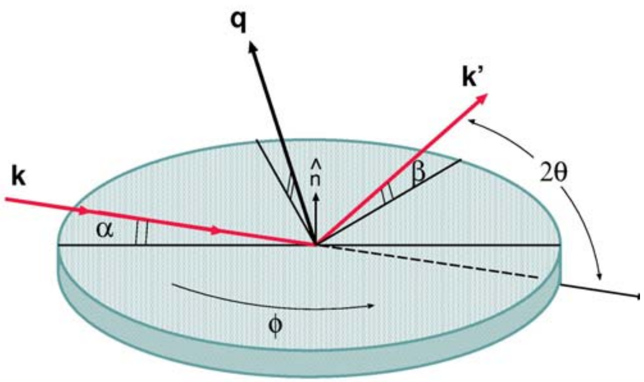


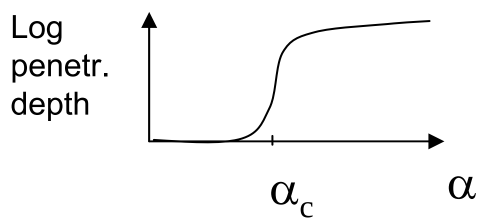


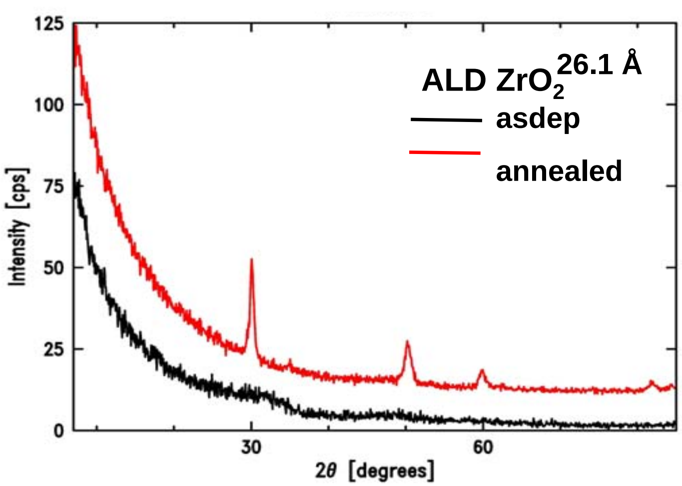


- Large beam footprint
- Eliminates thickness broadening
- Measures in-plane lattice parameters
- In-plane grain sizes
- H-K reciprocal space maps
- Phase ID of polycrystalline samples
- Can measure down to ~2 nm films
- Depth profiling

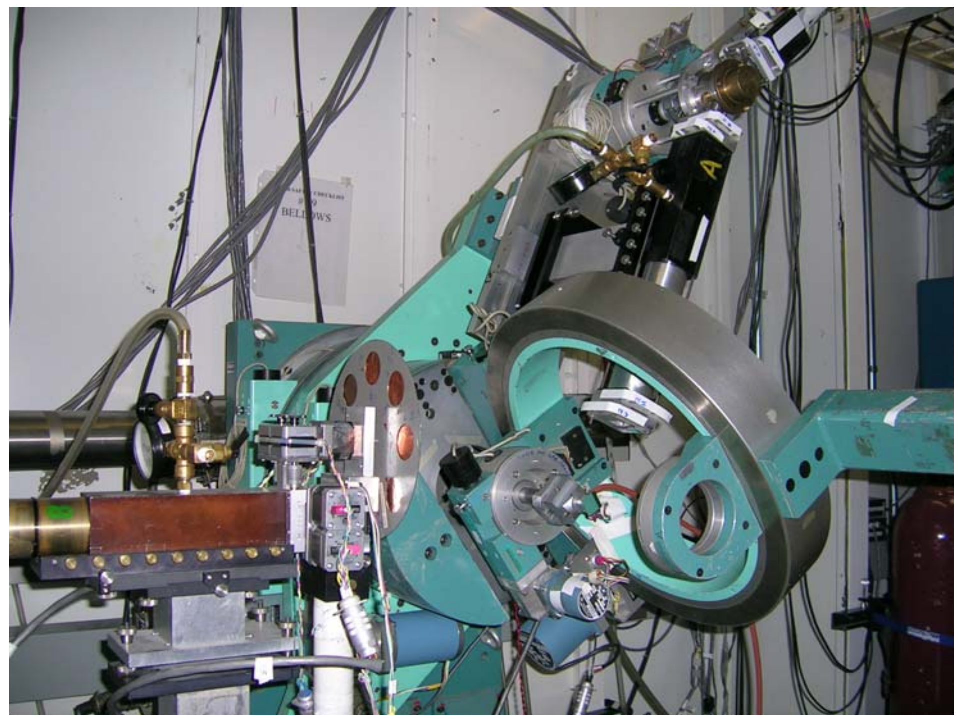

# Pt contacts on diamond: Grain size and texture

**Measurement:**

- GIXD: 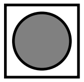

  h-scan (θ-2θ scan in grazing condition) with high-resolution (triple-axis) setup

  $\lambda$ = 1.54 Å, $FWHM_{Si111}$ = 0.008°2θ, $\alpha = \beta$ = 0.84º

  Eliminates thickness broadening

- Symmetric (Bragg-Brentano geometry):

  check for texture, compare with GIXD grain size measurem

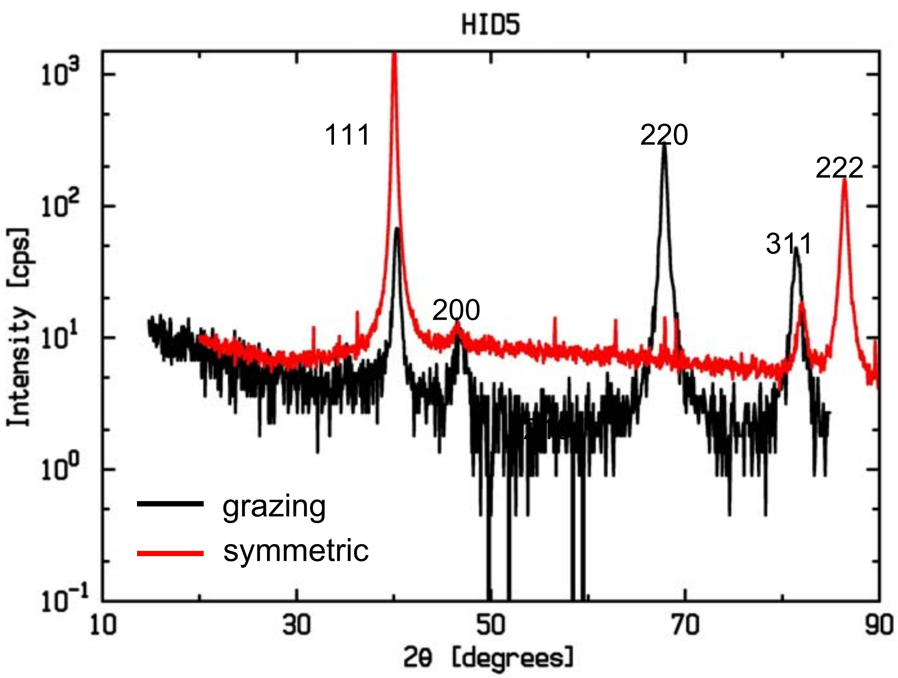


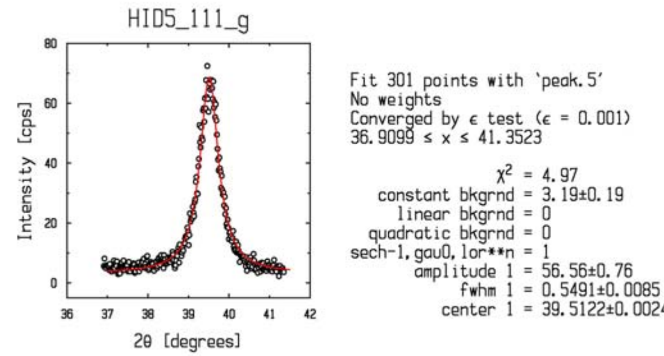


Scherrer formula for volume-averaged crystallite size: $D_v = K\lambda/\{\beta \cos \theta\}$

(Max ~ 4000Å)

| 111 fiber | grains | "random" | grains |
|---|---|---|---|
| 111s | 204 | 200s | 74 |
| 220g | 139 | 311s | 93 |
| | | 200g | 70 |
| | | 311g | 91 |

***Strong 111 fiber texture***

*www.chemistry.ohio-state.edu/~**woodward**/size_str.pdf*

# Stress Gradients induced in Cu films by capping layers

- Current-generation microelectronic technology employs electroplated Cu metallization.
- **Processing involved in creating metallization features requires thermal excursions that can induce strain in the Cu.**
- Interface between the Cu and capping layers represents a location that is susceptible to electromigration-induced mass flow. Stress state in this region is critical.

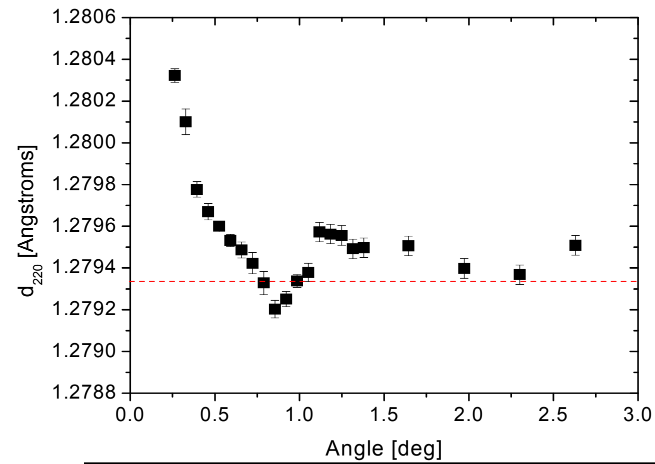


Measured Cu (220) reflection vs. incidence angle for $SiC_xN_yH_z$-capped Cu film. Dotted line refers to extrapolated in-plane bulk value (1.2793 Å).

## Results:

Grazing-incidence and conventional X-ray diffraction measurements determined the in-plane stress for Cu films having three different capping layers, as a function of depth. Cu films possessing a $SiC_xN_yH_z$ capping layer exhibited greater tensile stress near the cap than in the bulk, whereas Cu films possessing a CoWP film did not show a gradient. The constraint imposed by the $SiC_xN_yH_z$ cap during the cooling process from the cap deposition temperature (350 ºC) leads to an increase in the in-plane stress of 180 MPa from the bulk value.

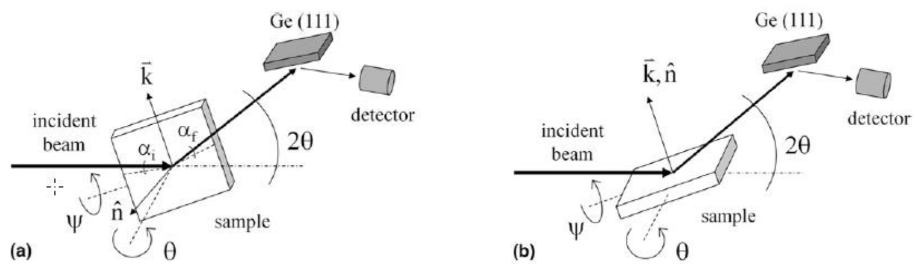


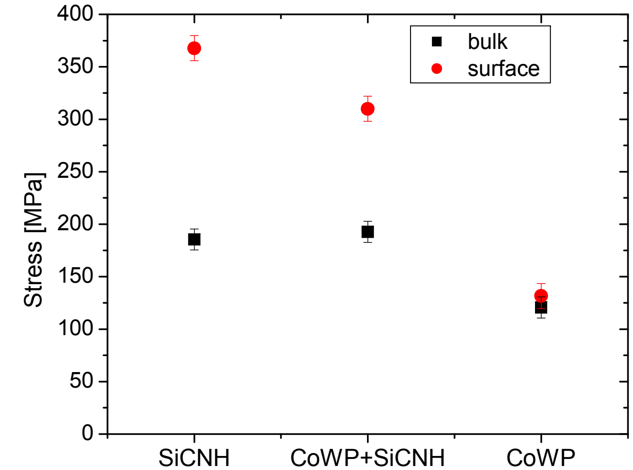


Comparison of in-plane stress values in Cu films in bulk and near-surface regions.

C.E. Murray et al., *Appl. Phys. Lett.* **93**, 221901 (2008); *J. Mat. Res.* **25**(4), 622 (2010)

# XRD Texture measurements: Pole-figures

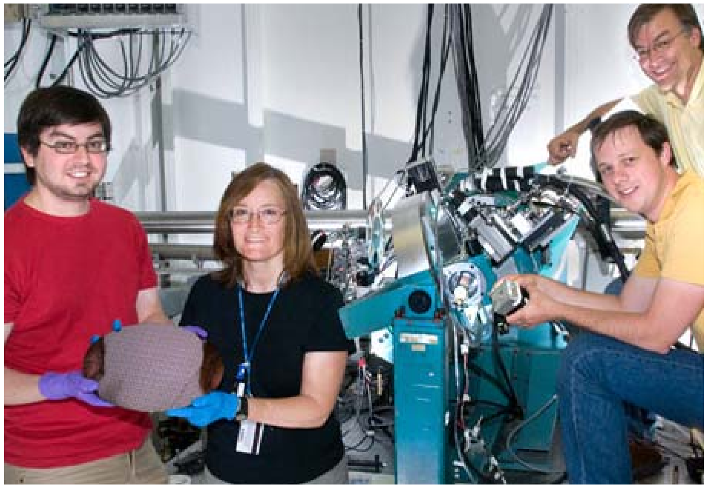

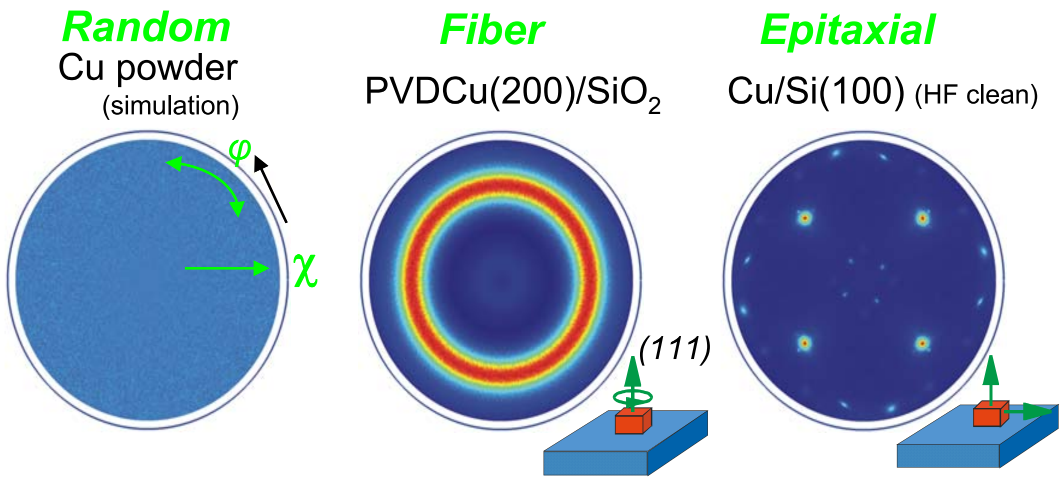


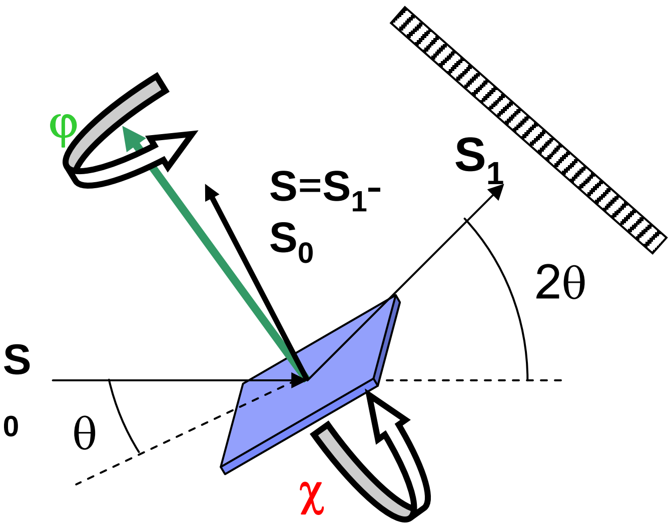


**TEXTURE OF THIN FILMS :**

- -Pole figures typically consist of simple geometric features
- -The features are frequently not very sharply defined
- -Pole figures for thin films are classified in 3 categories
  - -Random
  - -Fiber
  - -'In-plane alignment' or 'epitaxial alignment'

# Specular Reflectivity

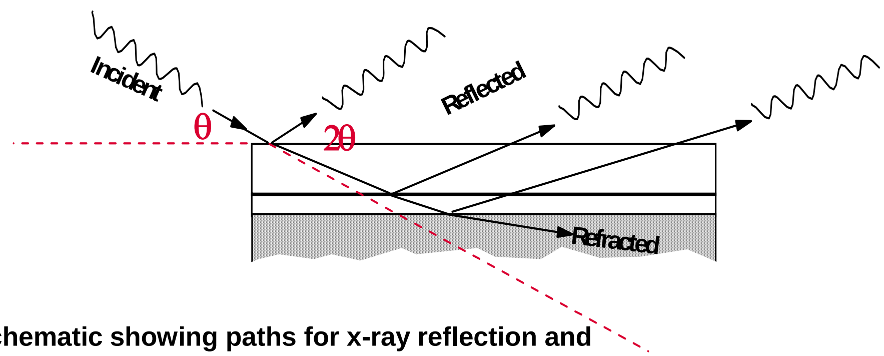


Schematic showing paths for x-ray reflection and refraction in a 2-layered film on a substrate

**TaN on Si after annealing to 550C**

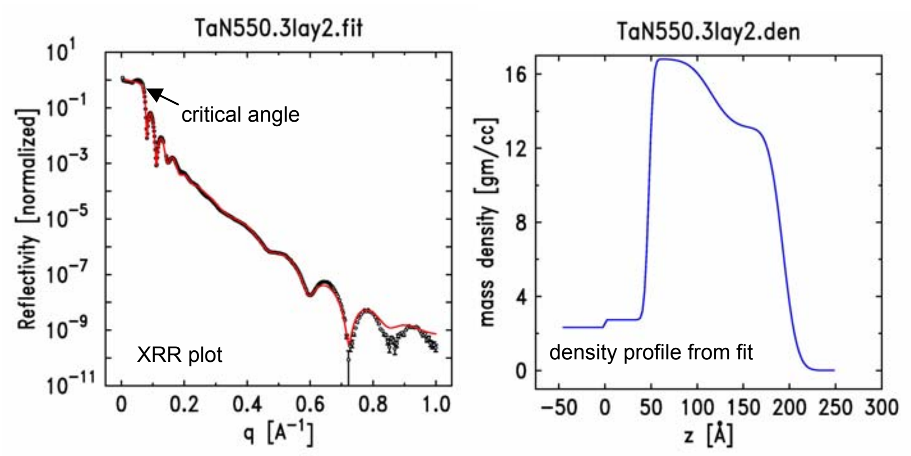


| Layer | Si | $SiO_2$ | TaN |
|---|---|---|---|
| σ (A) | 0.89 | 3.80 | 12.22 |
| t (A) | inf. | 47.58 | 145.28 |
| ρ (norm) | 1 | 1.094 | 0.91 |

- Crystalline or amorphous materials
- Model to obtain
  - thickness
  - density
  - roughness

  of each layer
- Thicknesses from ~20 – 2000 Å
- Can be difficult if
  - many layers
  - close in density
  - close in thickness

Variable T chamber on X20: RT to ~550°C

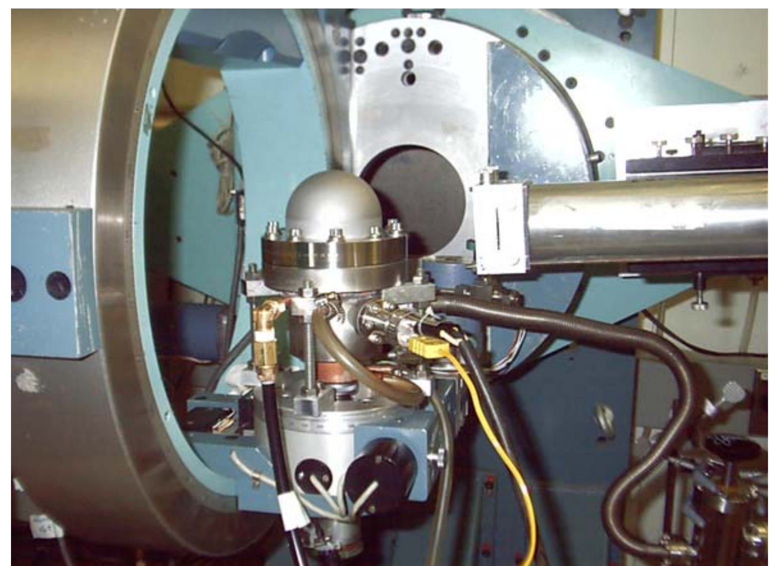

# Time- and Temperature-resolved *in-situ* XRD

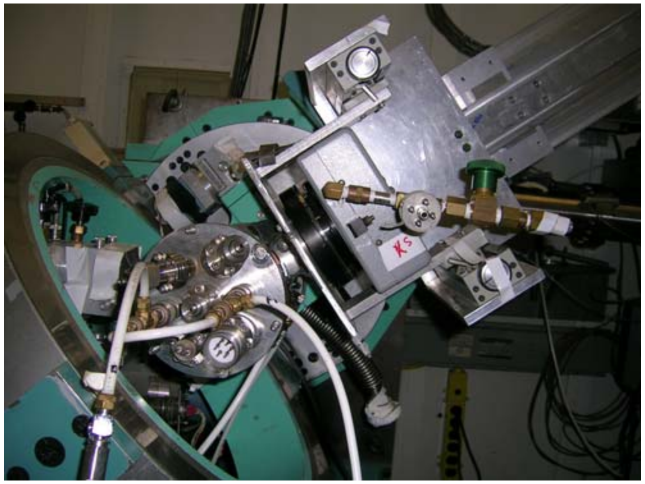

**RTA chamber on NSLS X20C beamline: *in-situ* time-resolved XRD, resistivity and light scattering**

- **Fast data collection and analysis**
- **Intense signal**
  - **Transformation temps**
  - **Morphology changes**
  - **Kinetics**
- **Quick evaluation of large array of variables**
  - **processes parameters**
  - **film thicknesses**
  - **dopants**
- **Size/scaling effects**

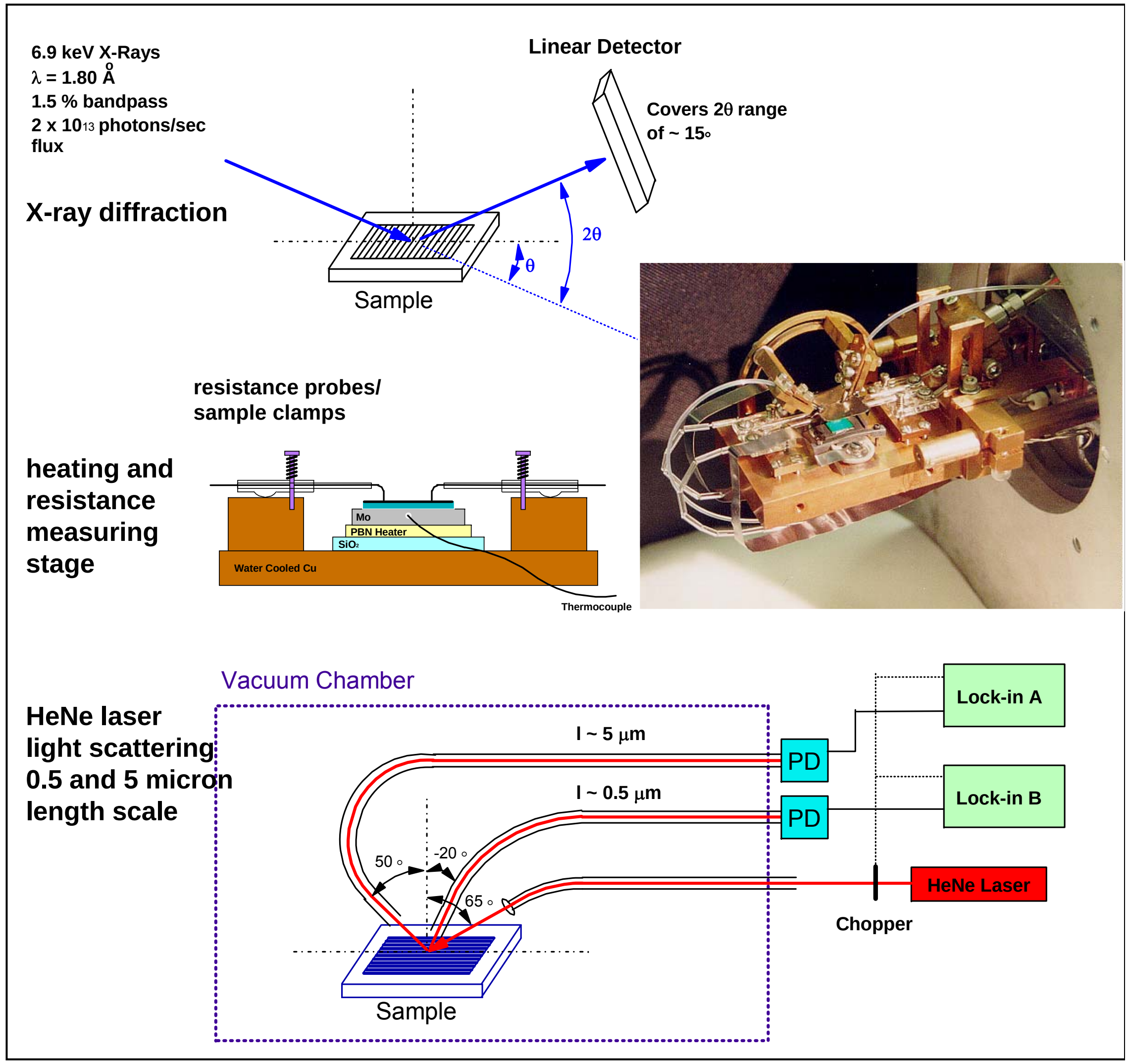


G.B. Stephenson *et al., Rev. Sci. Instrum*. **60**, 1537 (1989)
C. Lavoie *et al., Mat. Res. Soc. Symp. Proc*. **406**, 163 (1996)

# Contacts to diamond: Mo carbide

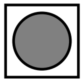

Detector-grade sc diamond
30 nm sputtered Mo,
3mm dia. both sides

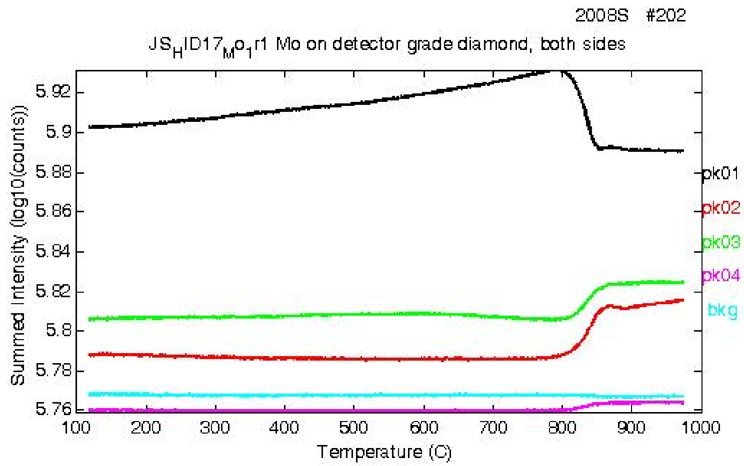


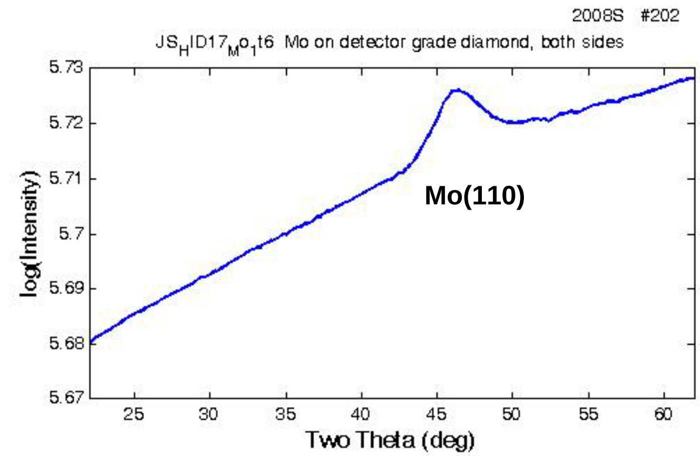


3C/s RTA to 1000C in He

*Formation temp = 835-840°C*

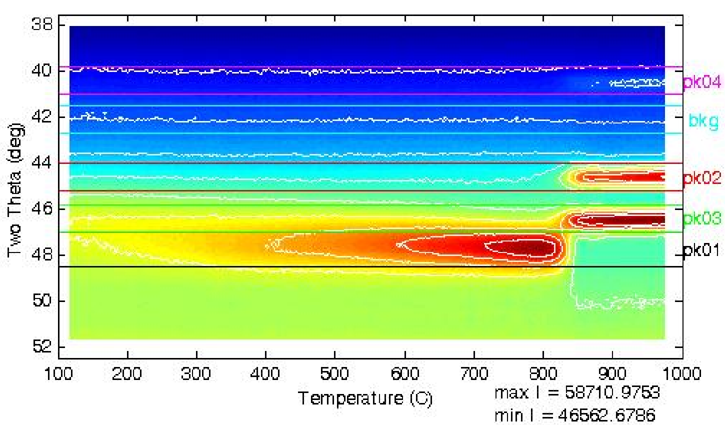


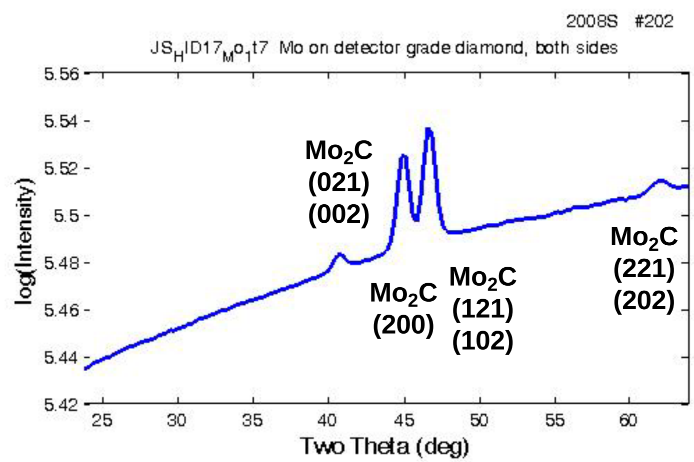

# Contacts to diamond: Pt

RTA 3C/s to 600C, fits

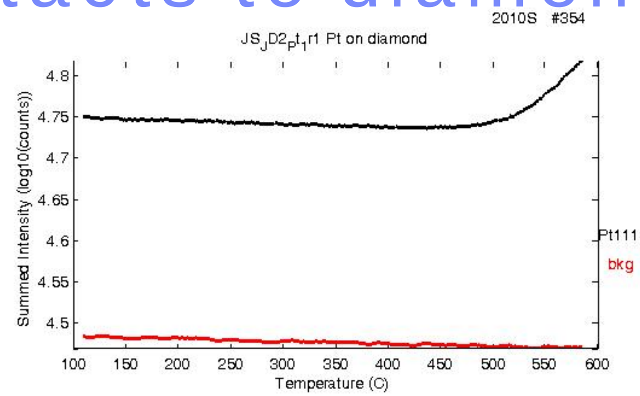


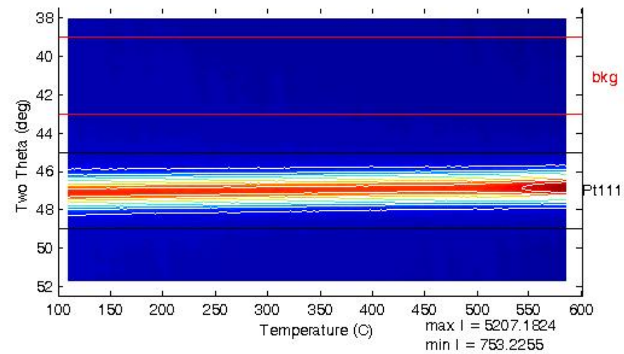


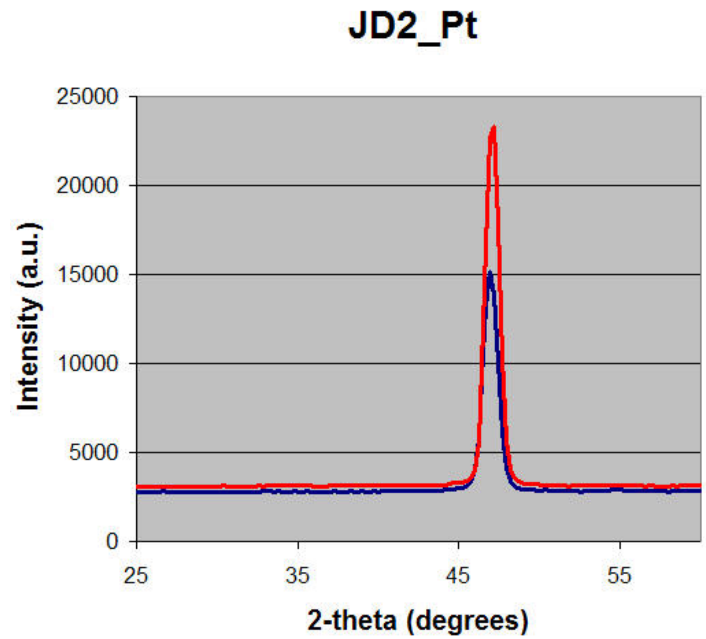


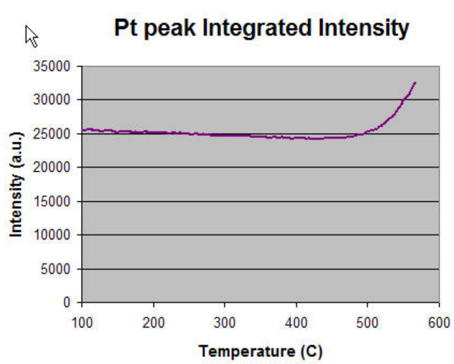


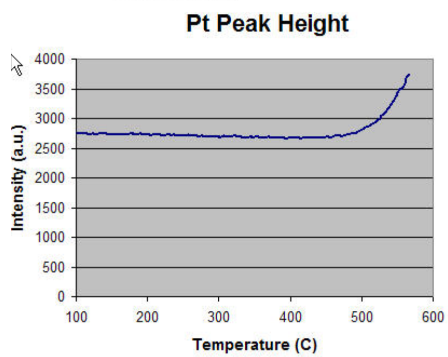


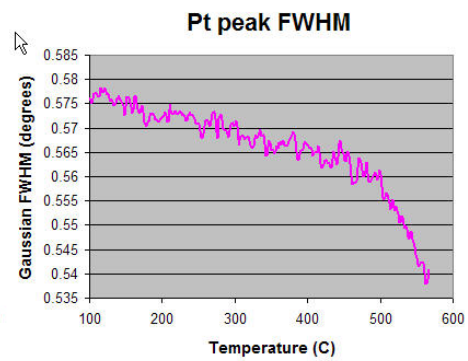


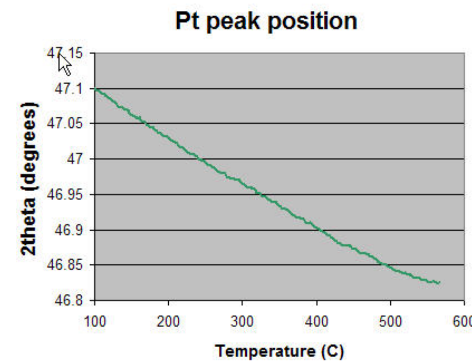

# Contacts to diamond: Pt

## isothermal 600C 5 min, fits

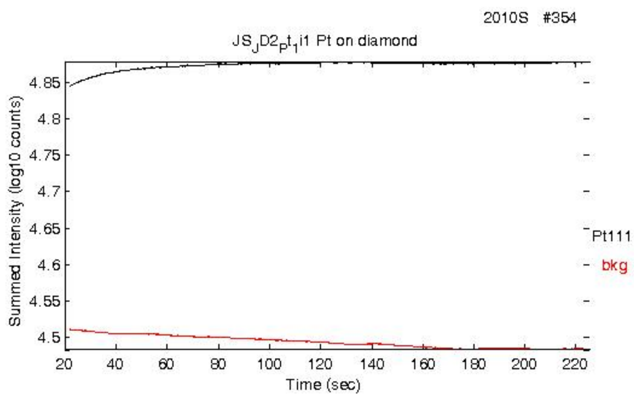


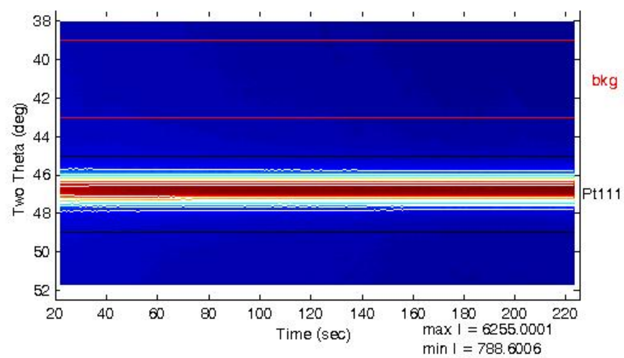


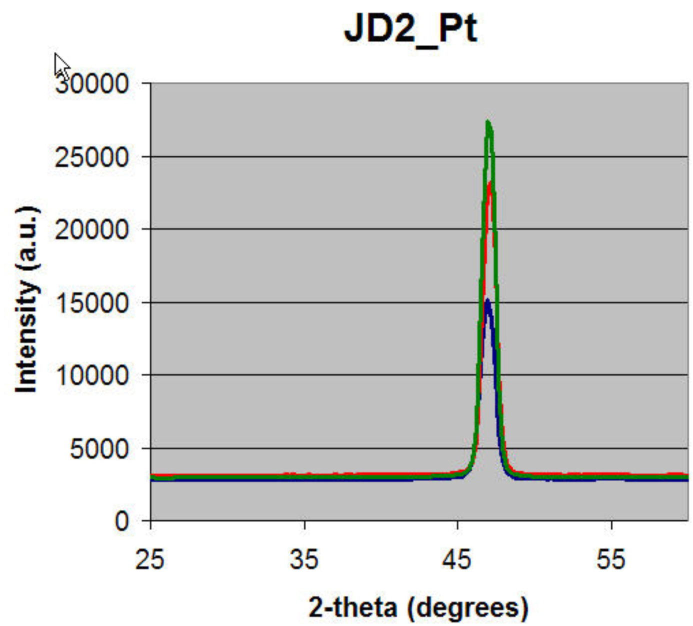


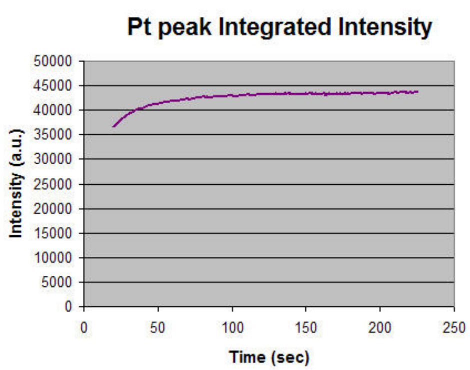


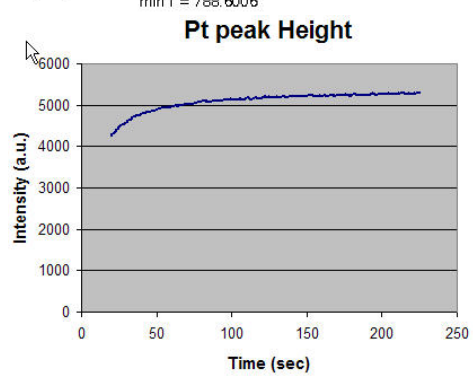


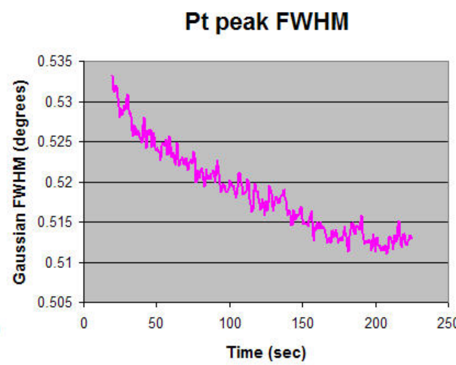


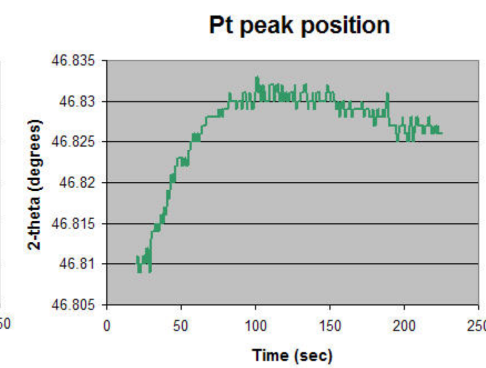

# Facility for Real-Time X-ray Studies of Thin Film and Surface Processes

## NSLS – Beamline X21

Experimental conditions can be optimized in chambers at the home laboratory …

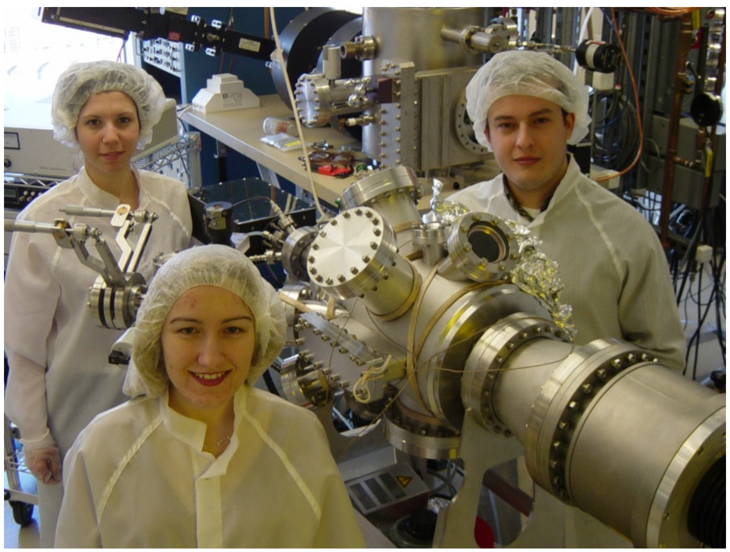

… the chambers can then be rolled onto the base diffractometer permanently installed at NSLS

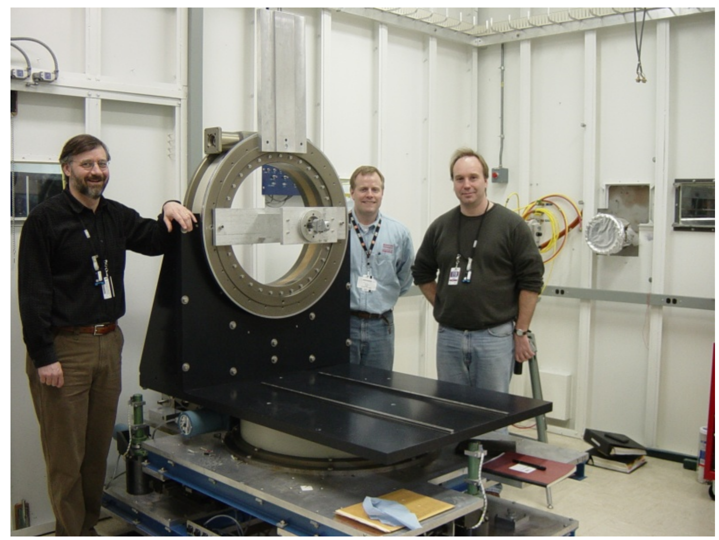

Diffractometer rail configuration compatible with CHESS G-line

BOSTON UNIVERSITY

# NSLS X21 Beamline

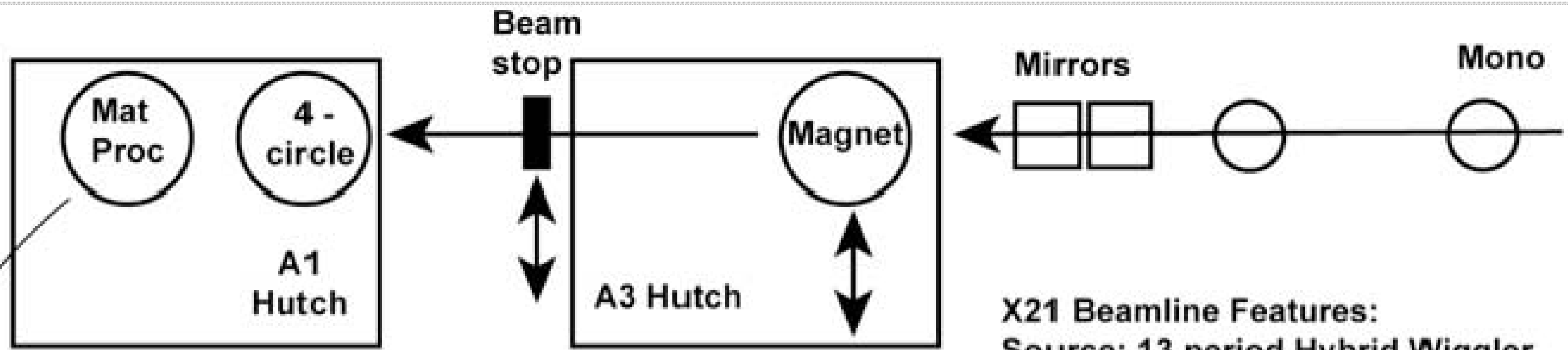


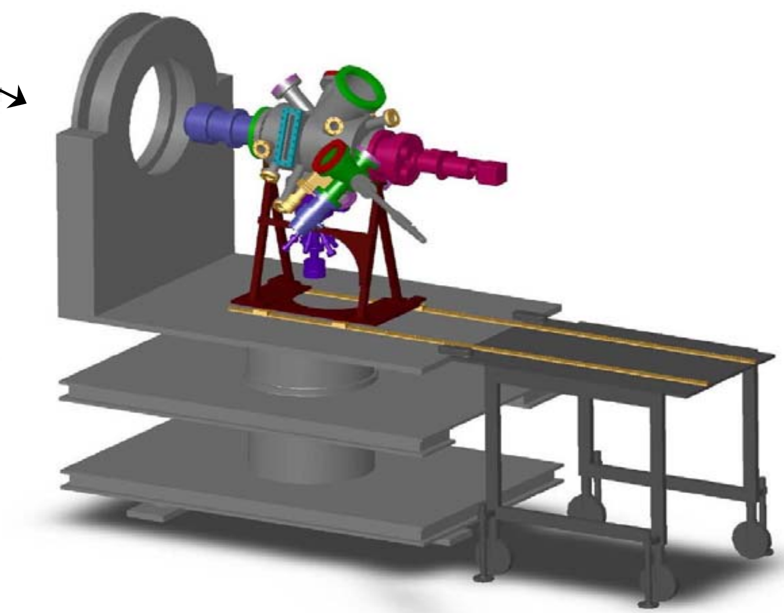

In-situ x-ray analysis system

X21 Beamline Features:
Source: 13 period Hybrid Wiggler
Energy Range: 5 -2 0 keV
Monochromators: Si(111) or
synthetic multilayer
Energy resolution: 1E-4 for Si(111).
Flux 2E12 ph/sec @ 300 mA with Si(111)

# Diffractometer Geometry

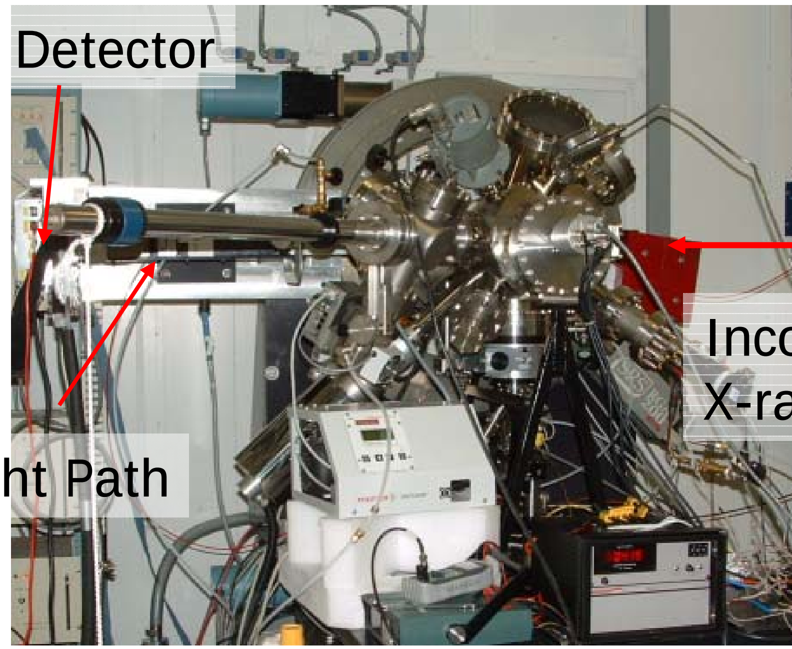


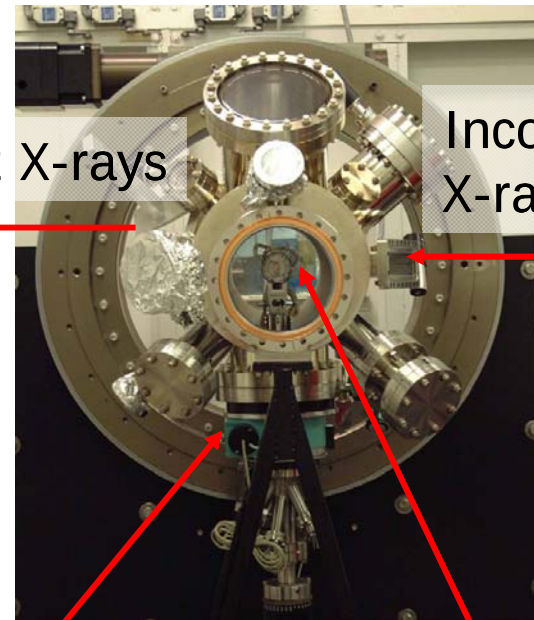


BOSTON UNIVERSITY

# Surface Modification and Characterization Instrumentation

**Boston U. Chamber:**

- Thermionics sample manipulator with BN heating element capable of heating samples to ~ 800 °C
- Oxford Scientific OSPrey ECR plasma source
- Applied Epi UNI-bulb RF plasma source
- Applied Epi SUMO effusion cells
- US Inc. sputter deposition source
- Balzers mass spectrometer
- Staib RHEED system
- Ircon infrared pyrometer

~ 50° access in-plane scans

~ 22° access out-of-plane scans

XRF, XRD, SAXS, XRR, GIXD, GISAXS, GIXOS

Plasma dep, sputter dep

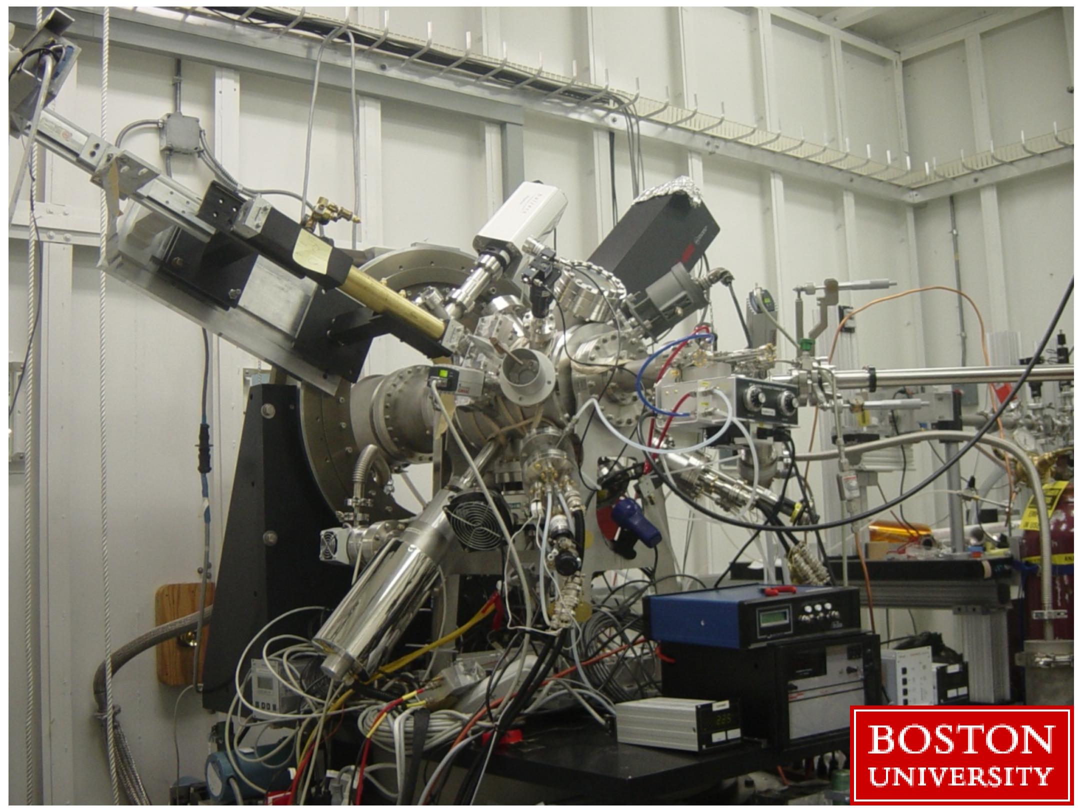

# Surface Modification and Characterization Instrumentation

**U. Vermont Chamber:**

Position sensitive linear detector.
Pilatus area detector.
RF Ion Source (100 - 1000 eV).
Phi Ion Gun (500 - 2000 eV)
Dual-gun Magnetron Sputter Deposition.
3 Effusion cells.
3 target Pulsed Laser Deposition

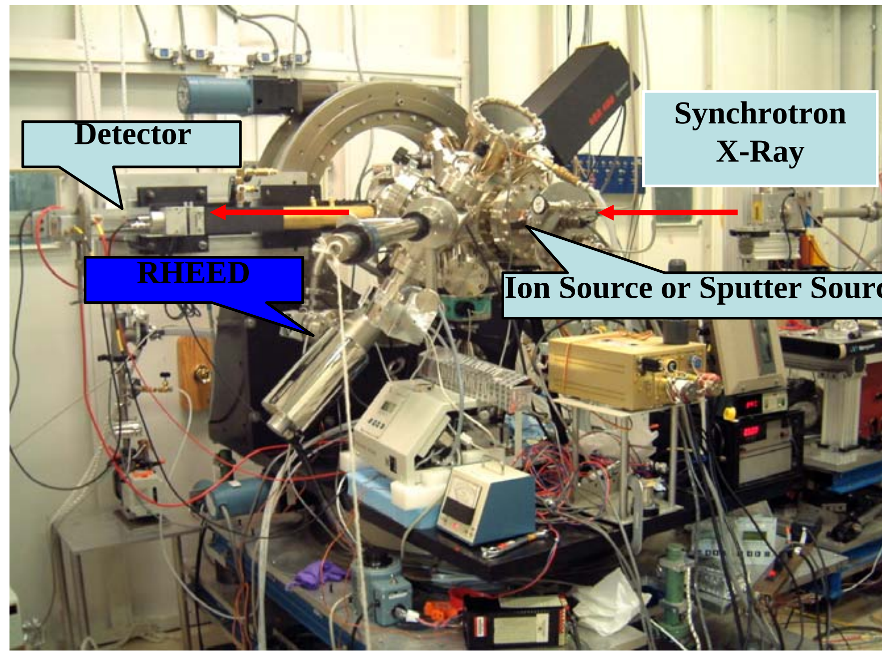


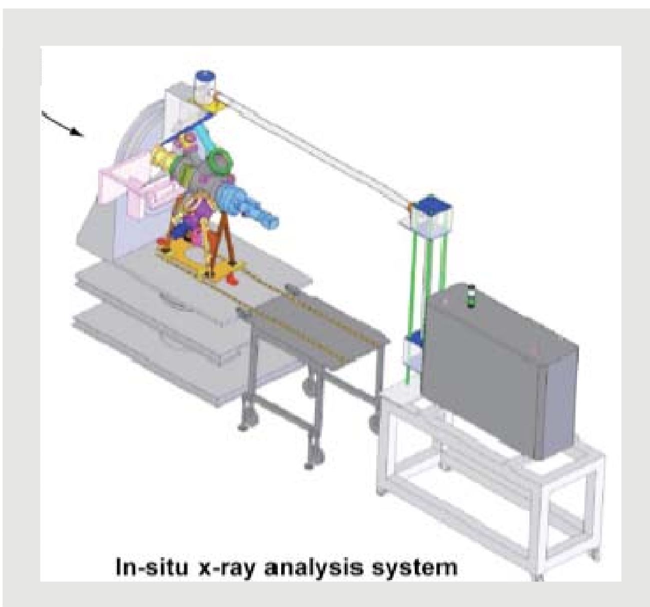
In-situ x-ray analysis system

XRF, XRD, SAXS, XRR,
GIXD, GISAXS, GIXOS

MBE, ALD, LPD, PVD, sputter dep

X-ray Studies of Materials with Analysis in Real Time Contributing User Team

The University of Vermont

# The Roll/On – Roll/Off chamber approach has been very productive at NSLS X21

- Surface Morphology Evolution during Ion Bombardment (Ludwig – BU)
- Plasma-Assisted MBE Growth of Nitrides (Ludwig – BU)
- Atomic Layer Deposition of $TiO_2$ (Detavernier Group – Ghent)
- Evolution of Surface Roughness during Multilayer Growth by Sputter Deposition (Headrick – UVt; Macrander – ANL)
- PLD of Semiconductors and Oxides (Headrick – UVt)
- Reactive Sputter Deposition of Oxides (Dawber – Stony Brook; Headrick – UVt)

For more information, contact Karl Ludwig (ludwig@buphys.bu.edu) or Randy Headrick (rheadrick@uvm.edu)

# Roughening and Stress Transitions in Sputter Deposition

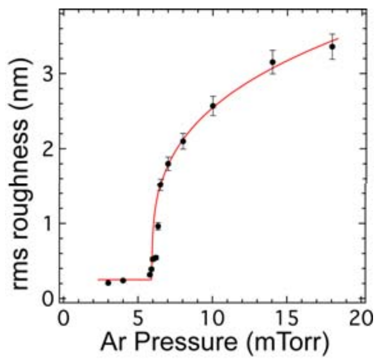


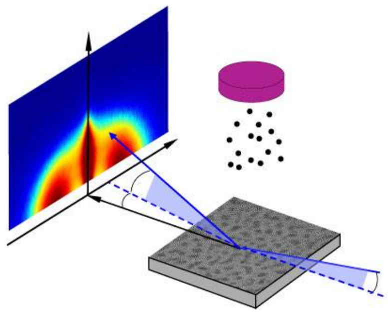

In-situ GISAXS

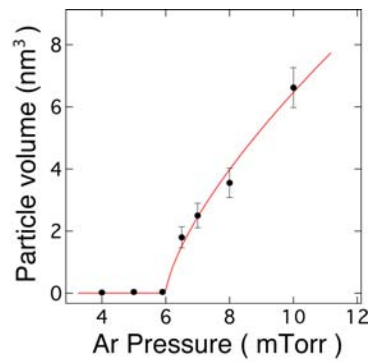


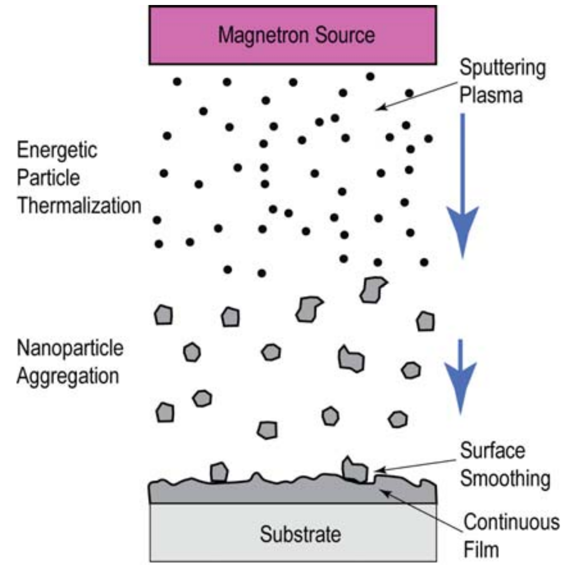


- This study resolves fundamental questions about the origin of stress and roughness in thin films formed by sputter deposition as the background gas pressure is increased beyond a threshold value.
- Film roughness and tensile stress are caused by formation of nanoparticles in the plasma/gas phase for Ar pressures above the threshold.
- Particle sizes for $WSi_2$ inferred from GISAXS spectra increase from ~1 atom at 6 mTorr to hundreds of atoms at 10 mTorr.

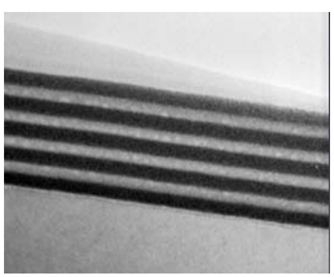

$WSi_2$/Si ML with 10 nm period deposited at 6 mTorr.

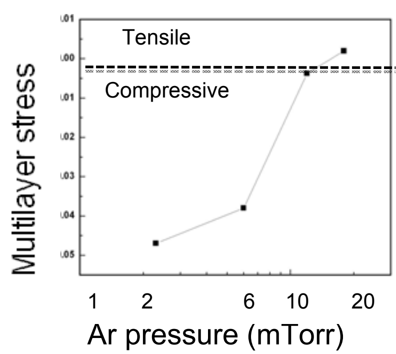


- In magnetron sputter deposition, collisions in the gas phase lead to the aggregation of nanoparticles.
- Nanoparticle formation is pressure dependent with a sharp onset at 6 mTorr for $WSi_2$.
- Particle size determines the roughening rate of amorphous thin films.
- Stress in $WSi_2$/Si multilayers deposited above the transition pressure becomes tensile when formed from nanoparticles due to particle coalescence and elimination of nano-voids.



Lan Zhou, Yiping Wang, Hua Zhou, Minghao Li, Randall L. Headrick, Kimberly Mac Arthur, Bing Shi, Ray Conley, and Albert T. Macrander
Phys. Rev. B, 82, 075408 (2010).